

# SCALABLE DECISION-MAKING IN STOCHASTIC ENVIRONMENTS THROUGH LEARNED TEMPORAL ABSTRACTION

**Anonymous authors**

Paper under double-blind review

## ABSTRACT

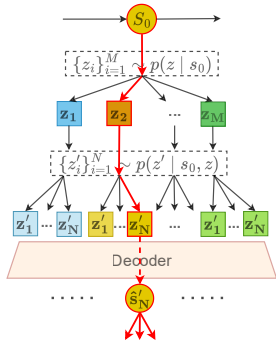
Sequential decision-making in high-dimensional continuous action spaces, particularly in stochastic environments, faces significant computational challenges. We explore this challenge in the traditional offline RL setting, where an agent must learn how to make decisions based on data collected through a stochastic behavior policy. We present *Latent Macro Action Planner* (L-MAP), which addresses this challenge by learning a set of temporally extended macro-actions through a state-conditional Vector Quantized Variational Autoencoder (VQ-VAE), effectively reducing action dimensionality. L-MAP employs a (separate) learned prior model that acts as a latent transition model and allows efficient sampling of plausible actions. During planning, our approach accounts for stochasticity in both the environment and the behavior policy by using Monte Carlo tree search (MCTS). In offline RL settings, including stochastic continuous control tasks, L-MAP efficiently searches over discrete latent actions to yield high expected returns. Empirical results demonstrate that L-MAP maintains low decision latency despite increased action dimensionality. Notably, across tasks ranging from continuous control with inherently stochastic dynamics to high-dimensional robotic hand manipulation, L-MAP significantly outperforms existing model-based methods and performs on-par with strong model-free actor-critic baselines, highlighting the effectiveness of the proposed approach in planning in complex and stochastic environments with high-dimensional action spaces.

## 1 INTRODUCTION

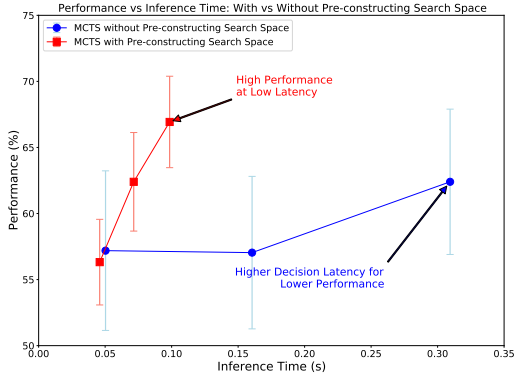
Planning-based reinforcement learning (RL) has achieved remarkable success in domains with discrete, low-dimensional action spaces, such as board games and video games (Silver et al., 2017; Schrittwieser et al., 2020; Ye et al., 2021), and continuous control tasks (Hubert et al., 2021; Schrittwieser et al., 2021). However, extending these methods to high-dimensional continuous action spaces, especially in stochastic environments, presents significant challenges. Many environments are inherently stochastic or appear stochastic to agents with limited capacity to model complex dynamics. For example, in autonomous driving, the behavior of other vehicles and pedestrians introduces substantial uncertainty that must be processed in real time (Carvalho et al., 2014). Recent planning-based offline RL approaches like Trajectory Transformer (Janner et al., 2021) face significant latency issues when trying to model and respond to these stochastic behaviors (Li et al., 2023). Similarly, in robotic manipulation, sensor noise introduces randomness that requires fast adaptive responses (Yang et al., 2023). In such cases, deterministic models often fail to capture the necessary randomness and intricacies (Antonoglou et al., 2022). Moreover, the vast and uncountable nature of continuous action spaces makes traditional planning approaches inefficient when operating directly in the raw action space (Jiang et al., 2023). These inefficiencies are further exacerbated in stochastic settings, leading to “large and long” planning problems where agents must manage numerous continuous variables over extended time horizons. This results in the *curse of dimensionality* and the *curse of history*, significantly hindering effective decision-making (Hubert et al., 2021).

In this paper, we posit that planning in such challenging settings could greatly benefit from temporal abstractions, i.e., representations of multi-step primitive behaviors such as macro actions (Dietterich, 2000; Sutton et al., 1999; Barto & Mahadevan, 2003). By leveraging these abstractions, planners

054  
055  
056  
057  
058  
059  
060  
061  
062  
063  
064  
065  
066  
067  
068  
069  
070  
071  
072  
073  
074  
075  
076  
077  
078  
079  
080  
081  
082  
083  
084  
085  
086  
087  
088  
089  
090  
091  
092  
093  
094  
095  
096  
097  
098  
099  
100  
101  
102  
103  
104  
105  
106  
107



(a) Planning with Pre-constructing search space



(b) Decision Latency vs. Performance

Figure 1: (a) Overview of planning over the pre-constructed search space. (b)As the number of MCTS iterations increases (10, 50, 100 from left to right), using a pre-constructed search space with MCTS achieves better performance with lower decision latency.

can navigate high-dimensional continuous action spaces more efficiently, potentially mitigating the curse of dimensionality and reducing decision-making latency in stochastic environments. This paper considers the standard setting where an agent can access a set of trajectories (i.e., a sequence of state, action, and reward traces) collected through a fixed behavior policy. Given this setting, we propose the *Latent Macro Action Planner* (L-MAP), which constructs a lower dimensional representation of temporally extended primitive actions by using a state-conditioned Vector Quantized Variational AutoEncoder (VQ-VAE) (van den Oord et al., 2017). The encoder integrates the current state and macro-action to generate a discrete latent code. Subsequently, we employ a Transformer to autoregressively model the distribution of these latent codes, conditioned on the current state (and the behavior policy). This Transformer facilitates a two-step inference process: initially, given a state, it enables the sampling of probable latent macro-actions under the behavior policy, effectively acting as a prior policy. Subsequently, conditioned on both the state and the sampled macro-action, it generates subsequent latent codes that encapsulate information about expected returns and potential next states. This dual functionality of the Transformer enables efficient exploration of promising action trajectories while forming a compact representation of the plausible trajectories during planning.

As shown in Fig.1a, leveraging these models, we build a latent search space that serves as a structured initialization for planning, encapsulating likely trajectories based on the learned environment dynamics. To address stochasticity and optimize decision-making, we integrate Monte Carlo Tree Search (MCTS) with progressive widening to efficiently navigate this latent space. Initially, the search concentrates on the prebuilt latent space, facilitating rapid decision-making grounded in learned abstractions. If additional computation time becomes available, we progressively widen the search tree to extend the search beyond the prebuilt latent space incrementally. This dynamic expansion strategy enables our method to balance rapid planning using learned abstractions with more exhaustive exploration when computational resources permit. Upon selecting a latent macro-action, we operate in a *polling control* mode (He et al., 2011; Gabor et al., 2019) wherein MCTS returns only the first primitive action of the recommended macro-action. This approach allows for recovery from locally suboptimal decisions by performing planning at each time step.

We evaluate L-MAP extensively in the offline RL setting across a diverse range of tasks. In stochastic MuJoCo environments (Rigter et al., 2023), L-MAP consistently outperforms both model-based baselines like Trajectory Transformer (TT) (Janner et al., 2021) and Trajectory Autoencoding Planner (TAP) (Jiang et al., 2023), as well as model-free methods such as Conservative Q-Learning (CQL) (Kumar et al., 2020) and Implicit Q-Learning (IQL) (Kostrikov et al., 2022). This demonstrates L-MAP’s robust capability in handling stochastic dynamics. For deterministic MuJoCo tasks, L-MAP shows comparable or superior performance to these baselines, highlighting that our planning approach effectively accounts for stochasticity in the behavior policy, leading to competitive performance even in deterministic environments. Notably, L-MAP scales effectively to high-dimensional tasks, as evidenced by its strong performance on the challenging Adroit hand manipulation tasks.

108 Furthermore, L-MAP’s use of temporal abstraction enables lower latency decision-making com-  
 109 pared to methods like TT. These results underscore L-MAP’s versatility and effectiveness across  
 110 various types of control problems, from stochastic to deterministic environments, and from low to  
 111 high-dimensional action spaces.

## 113 2 PRELIMINARIES

115 We consider a continuous state and action space Markov Decision Process (MDP) defined by  
 116  $\{\mathcal{S}, \mathcal{A}, P, r\}$ , where  $\mathcal{S} \subseteq \mathbb{R}^n$  is the state space,  $\mathcal{A} \subseteq \mathbb{R}^l$  is the action space,  $P : \mathcal{S} \times \mathcal{A} \rightarrow \Delta(\mathcal{S})$  is  
 117 the transition function, and  $r : \mathcal{S} \times \mathcal{A} \rightarrow \mathbb{R}$  is the reward function. To manage the complexity of  
 118 these continuous spaces, we introduce macro actions, which are fixed-length sequences of primitive  
 119 actions. A macro action  $m \in \mathcal{M}$  is defined as  $m = \langle a_t, \dots, a_{t+L-1} \rangle$ , where each  $a_i \in \mathcal{A}$  and  $L$  is  
 120 the length of the macro action. Our goal is to compute an optimal macro-level policy  $\pi^* : \mathcal{S} \rightarrow \mathcal{P}_m$   
 121 that maximizes the expected discounted return  $\mathbb{E}_\pi [R(s, \pi(s))]$ .

122 **Trajectory Representation:** Consider a trajectory  $\tau$  of length  $T = \kappa \cdot L$  ( $\kappa \in \mathbb{N}^+$ ),  
 123 which is composed of a sequence of states  $s_t \in \mathcal{S}$ , fixed-size macro actions  $m_t \in \mathcal{M}$ ,  
 124 and corresponding return-to-go estimates  $R_t = \sum_{i=t}^T \gamma^{i-t} r_i$ , formally represented as  $\tau =$   
 125  $(R_1, s_1, m_1, R_{L+1}, s_{L+1}, m_{L+1}, \dots, R_{(\kappa-1)L+1}, s_{(\kappa-1)L+1}, m_{(\kappa-1)L+1})$ .

## 127 3 METHOD

128 Planning in continuous action space is hard and computationally challenging, and full enumera-  
 129 tion of all possible actions is infeasible. Discretizing the action space is one way to address this  
 130 challenge, but in practice, enumerating a large set of discrete actions can also be challenging, particu-  
 131 larly for online approaches. Sample-based methods offer an efficient approach for handling large  
 132 and complex domains. These methods sample a subset of actions rather than exhaustively enum-  
 133 erating all possibilities, reducing computational costs while computing optimal policies or value  
 134 functions (Hubert et al., 2021). Building on these insights, we propose the Latent Macro Action  
 135 Planner (L-MAP), which learns temporal abstractions in the form of macro-actions and plans using  
 136 a latent transition model that serves as both a prior policy and a transition model.

### 138 3.1 DISCRETIZING STATE-MACRO ACTION SEQUENCES WITH VQ-VAE

139 A key insight from prior work is that a learned state-conditioned discretization can be used to con-  
 140 struct a discretization scheme with relatively few discrete actions while maintaining high granu-  
 141 larity (Jiang et al., 2023; Luo et al., 2023). As shown in Fig.2, Our approach leverages a learned  
 142 state-conditioned discretization to enable planning in a lower-dimensional discrete space. Specifi-  
 143 cally, our encoder processes sequences of state and macro-actions as input. For example, each token  
 144 is defined as  $x_t = (R_t, s_t, m_t)$  and its subsequent token as  $x_{t+L} = (R_{t+L}, s_{t+L}, m_{t+L})$ . The  
 145 encoder function is defined as:

$$146 f_{\text{enc}}(x_t = (R_t, s_t, m_t), x_{t+L} = (R_{t+L}, s_{t+L}, m_{t+L})) = (z_t, z_{t+L}), \quad (1)$$

147 where the transition chunk size is two, resulting in two latent codes assigned per chunk. To elaborate,  
 148 the encoder first concatenates the input return-to-go estimates, states, and macro actions into two  
 149 transition vectors. It then applies a sequence model, in our case, a causal Transformer, producing  
 150 two latent feature vectors for each chunk of transitions.

151 In stochastic environments, executing the same macro-action  $m$  from state  $s$  can yield different  
 152 returns  $R$ , introducing variability that complicates the vector quantization in VQ-VAE, i.e., note that  
 153 using the full token  $x_t = (R_t, s_t, m_t)$  directly can result in different latent codes  $z$  for identical  
 154  $(s_t, m_t)$  pairs solely due to differences in  $R_t$ . This challenge can cause the latent space to become  
 155 fragmented and reflect return variability more than the underlying structure of available actions.  
 156 Consequently, the agent might overestimate the returns during decision-making by emphasizing  
 157 latent codes associated with higher observed returns, neglecting the true distribution of the primitive  
 158 actions and their expected returns.

159 To address this issue, we aim to focus the vector quantization process primarily on representations  
 160 of the state  $s$  and macro-actions  $m$ , while still preserving the ability to reconstruct the return  $R$ . A  
 161

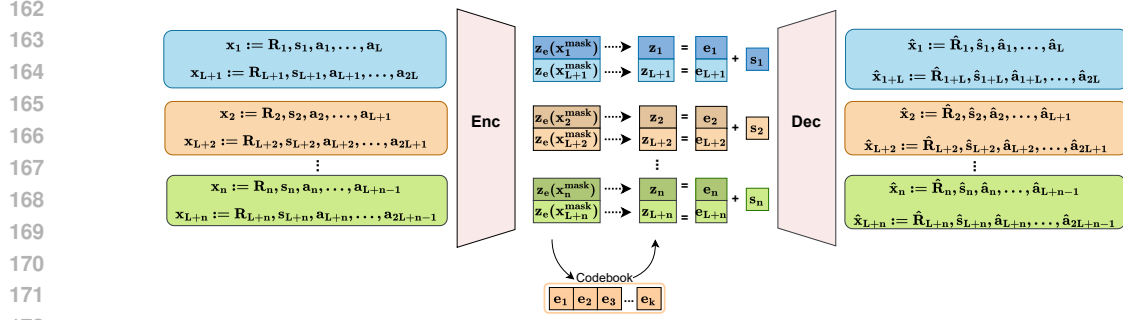


Figure 2: An overview of our VQ-VAE model that discretizes state-macro action sequences

simple approach to achieve this would be to mask the return signal  $R$  in the input (i.e., only include  $s$  and  $m$ ) and train a model to reconstruct the full token (i.e.,  $\hat{R}$ ,  $s$  and  $m$ ). We tested this approach in initial experiments but received poor convergence, indicating that the model was not effectively capturing the necessary information to reconstruct  $x$ .

To tackle this challenge, our approach involves creating two versions of each token  $x_t$ : the full input  $x_t = (R_t, s_t, m_t)$  and a masked version  $x_t^{\text{mask}} = (\text{mask}, s_t, m_t)$ , where  $R_t$  is masked out. The encoder processes both  $x_t$  and  $x_t^{\text{mask}}$  to generate two embeddings,  $z_e(x_t)$  and  $z_e(x_t^{\text{mask}})$ , respectively. We use  $z_e(x_t^{\text{mask}})$  for vector quantization to obtain the quantized latent code  $z_q(x_t^{\text{mask}})$ . To ensure that the codebook embeddings incorporate information from the full input, including  $R_t$ , we update the embedding  $e_t$  of the quantized latent code towards  $z_e(x_t)$ . We modify the loss function by introducing an additional term that encourages the embedding from the masked input to be close to that from the full input. Specifically, we used the embedding from the full input  $z_e(x)$  as the learning target for the embedding of the masked input  $z_e(x^{\text{mask}})$ . The modified loss function is:

$$\mathcal{L} = \log p(x | z_q(x^{\text{mask}})) + \|\text{sg}[z_e(x)] - e\|_2^2 + \beta \|z_e(x^{\text{mask}}) - \text{sg}[e]\|_2^2 + \|z_e(x^{\text{mask}}) - z_e(x)\|_2^2 \quad (2)$$

where  $\text{sg}$  denotes the stopgradient operator and the additional term  $\|z_e(x^{\text{mask}}) - z_e(x)\|_2^2$  acts as a regularizer that aligns the embeddings of the masked and full inputs.

Incorporating macro-actions within each token is critical, as it enables the model to capture temporal dependencies across multiple time steps without the need for downsampling. This approach is particularly important in stochastic settings, where downsampling techniques that aggregate states (as in Jiang et al. (2023)) can obscure the stochasticity imposed by the environment’s dynamics. The decoder takes the initial state and latent codes as inputs, and outputs the reconstructed trajectories:

$$f_{\text{dec}}(s_t, z_t, z_{t+L}) = (\hat{x}_t = (\hat{R}_t, \hat{s}_t, \hat{m}_t), \hat{x}_{t+L} = (\hat{R}_{t+L}, \hat{s}_{t+L}, \hat{m}_{t+L})). \quad (3)$$

The decoding process can be seen as the inverse of the encoding process, except that the initial state  $s_t$  is merged into the embeddings of the codes with a linear projection before decoding.

**Latent Transition Model:** Following the discretization process, the subsequent step involves modeling sequences of latent codes in an autoregressive manner using a causal Transformer. The Prior Transformer is conditioned on the initial state  $s_t$ , achieved by adding the state feature to all token embeddings. Primarily, it functions as a transition model in the latent space, enabling the sampling of the next latent code  $z_{i+1}$  conditioned on the current code  $z_i$  and state  $s$ . This transition, represented as  $T : \mathcal{S} \times \mathcal{Z} \rightarrow \mathcal{Z}$ , implicitly captures the full  $\mathcal{R} \times \mathcal{S} \times \mathcal{M} \rightarrow \mathcal{R} \times \mathcal{S} \times \mathcal{M}$  transition in the original space, as each  $z$  encodes information about the return-to-go, state and macro-action. Additionally,  $p(z | s)$  acts as a prior policy for efficient action sampling, allowing rapid selection of probable macro-actions based on learned behaviors from the offline dataset. By operating in the learned latent space, the model potentially reduces computational complexity compared to modeling transitions in the original state-action space, especially for high-dimensional environments. The discrete nature of the latent space allows for efficient sampling, which can be beneficial for downstream tasks such as planning.

### 3.2 PLANNING WITH A LATENT MACRO ACTION MODEL

Planning in high-dimensional environments using learned discrete representations introduces uncertainties from multiple sources. First, the representation learning process introduces uncertainty due to the non-injective mapping from the high-dimensional state-action space to a lower-dimensional latent space. This can result in many-to-one correspondences, where multiple distinct high-dimensional inputs map to the same latent representation, creating apparent stochasticity even in deterministic environments. Second, the environment itself may be inherently stochastic.

We argue that taking expectations over latent transitions is beneficial in mitigating all these sources of uncertainty, regardless of whether the environment is deterministic or stochastic. By considering the expected outcomes over multiple latent transitions, we can average out the randomness introduced by the non-injective mapping and inherent stochasticity, leading to more reliable planning decisions. This insight applies broadly to planning methods that employ models with non-injective mapping characteristics. Building on this insight, we employ Monte Carlo Tree Search (MCTS) as our planning algorithm to mitigate the impact of stochasticity arising from non-injective mappings and potential environmental randomness. MCTS iteratively explores the latent space and takes expectations over transitions, allowing for robust planning in the presence of uncertainty.

**Pre-constructing the Latent Search Space** Our approach leverages a learned latent transition model to generate and evaluate macro actions for planning efficiently. Starting from an initial state  $s_0$ , we sample  $M$  latent codes  $z$ , each representing a potential macro action. For each sampled latent code  $z$ , we sample  $N$  subsequent latent codes  $z'$  to simulate possible future trajectories, capturing the outcomes of these macro actions. We obtain the corresponding state-action transitions and return estimates by decoding these latent pairs  $(z, z')$  conditioned on  $s$ .

To construct the planning tree efficiently, we cache the initial state  $s_0$  along with the top- $k$  latent codes  $z$  (and their associated information) based on the decoded returns, where  $k = \lambda \times M$  and  $\lambda \in (0, 1]$  controls the expansion ratio of the tree. The cached latent codes represent the most promising macro actions to consider from the initial state. The latent codes  $z'$  are then decoded to obtain a set of reconstructed tokens, i.e.,  $(R, s, m)$ . For each of these states  $s$ , we sample  $B$  latent codes  $z''$ , representing potential macro actions from  $s$  (note that  $B$  and  $M$  are exogenously defined hyper-parameters).

This process is recursively applied, allowing us to expand the planning tree while controlling its growth through the parameter  $\lambda$ . By focusing on the most promising macro actions at each state, we maintain a compact and informative planning structure that efficiently explores the state-action space at a macro level.

**Selection.** Starting from the cached tree structure, MCTS iteratively expands and evaluates nodes, allowing for a more comprehensive exploration of the state-action space. For each state  $s$  in the tree, MCTS selects one of the top- $k$  cached latent codes  $z$  based on the Upper Confidence Bounds for Trees (UCT) (Kocsis & Szepesvári, 2006):  $UCT(s, z) = Q(s, z) + c\sqrt{\frac{\log(N(s))}{N(s, z)}}$  where  $Q(s, z)$  represents the value of executing macro action  $z$  in state  $s$  (estimated through the decoded return-to-go),  $N(s)$  denotes the number of times state  $s$  has been visited,  $N(s, z)$  denotes the number of times macro action  $z$  has been chosen in state  $s$ , and  $c$  is an exploration coefficient.

**Progressively Widening the State Space for Search:** Despite these powerful abstraction techniques, the search space remains challenging due to the underlying high-dimensional nature of the

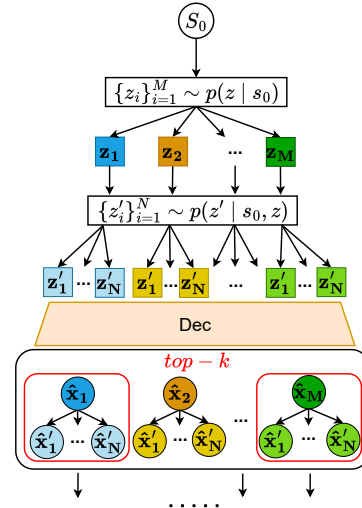


Figure 3: Pre-construction of the latent search space by sampling and evaluating latent macro-action codes, caching the top- $k$  candidates, and recursively expanding the planning tree for efficient macro-level planning.

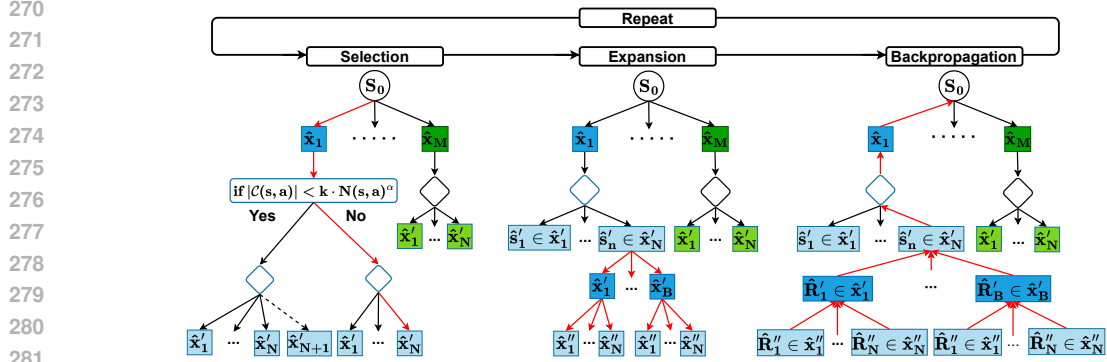


Figure 4: Illustration of our MCTS process for macro-level planning. The algorithm iteratively selects actions using the UCT policy, applies progressive widening to balance exploration and exploitation, performs parallel expansion of multiple macro actions and their potential outcomes, and backpropagates estimated Q-values to efficiently explore and refine the planning tree.

original state space, residual stochastic characteristics of transitions in the abstracted space, and the complexity of long-horizon planning scenarios. If we were to apply MCTS directly to this abstracted space, we would encounter two main issues: inefficient utilization of our pre-built search space, with the search potentially diverging prematurely into unexplored regions, and difficulty in building sufficiently deep trees for high-quality long-term decision-making, particularly in areas of high stochasticity or uncertainty (Couëtoux et al., 2011). Therefore, we use progressive widening to extend MCTS to incrementally expand the search tree. It balances the exploration of new states with the exploitation of already visited states based on two hyperparameters:  $\alpha \in [0, 1]$  and  $\epsilon \in \mathbb{R}^+$ . Let  $|\mathcal{C}(s, z)|$  denote the number of children for the state-action pair  $(s, z)$ . The key idea is to alternate between adding new child nodes and selecting among existing child nodes, depending on the number of times a state-action pair  $(s, z)$  has been visited. A new state is added to the tree if  $|\mathcal{C}(s, z)| < \epsilon \cdot N(s, z)^\alpha$ , where  $N(s, z)$  is the number of times the state-action pair has been visited. The hyperparameter  $\alpha$  controls the propensity to select among existing children, with  $\alpha = 0$  leading to always selecting among existing child and  $\alpha = 1$  leading to vanilla MCTS behavior (always adding a new child). In this way, we could enhance our approach by efficiently utilizing the pre-built search space, prioritizing the exploration of promising macro actions while allowing for incremental expansion of the search tree. This technique enables our method to make quick decisions in an anytime manner, leveraging the cached information, and further refine the planning tree if additional time is available.

**Expansion.** In our approach, the *expansion* phase differs from standard MCTS by performing *parallel expansion* of multiple nodes from a leaf node. From the leaf node, a set of  $B$  latent codes  $\{z^{(i)}\}_{i=1}^B$  is sampled, each representing a distinct macro action, drawn from a latent transition model  $p(z | s)$  to ensure diverse action space coverage. For each sampled macro action  $z^{(i)}$ ,  $N$  subsequent latent codes  $\{z^{(i,j)}\}_{j=1}^N$  are sampled according to  $z^{(i,j)} \sim p(z' | z^{(i)}, s)$ , for  $j = \{1, \dots, N\}$ , modeling potential outcomes and capturing the stochastic nature of macro actions. These latent transitions are then decoded to obtain the resulting next states  $\{s^{(i,j)}\}_{j=1}^N$  for each macro action. Finally, the search tree is expanded by adding all  $L$  child nodes  $\{(s^{(i,j)}, z^{(i,j)})\}_{j=1}^N$  for each macro action  $z^{(i)}$  to the current leaf node  $s$ . This breadth-wise expansion enables simultaneous exploration of multiple promising macro actions, enhancing the diversity and comprehensiveness of the search and facilitating efficient exploration in complex environments.

**Backpropagation.** Following the expansion phase, where multiple macro actions are expanded simultaneously, the *backpropagation* step updates the estimated Q-values based on the return-to-go as shown in Fig.4.

## 4 EXPERIMENTS

The empirical evaluation of L-MAP consists of three sets of tasks from D4RL (Fu et al., 2020): gym locomotion control, AntMaze, and Adroit. We compare L-MAP to a range of prior offline RL



algorithms, including both model-free actor-critic methods (Kumar et al., 2020; Kostrikov et al., 2022) and model-based approaches (Rigter et al., 2023; Jiang et al., 2023; Janner et al., 2021). Our work is conceptually most related to the Trajectory Transformer (TT; Janner et al. (2021)) and the Trajectory Autoencoding Planner (TAP; Jiang et al. (2023)), which are model-based planning methods that predict and plan in continuous state and action spaces. These two baselines serve as our main points of comparison for deterministic environments.

To demonstrate L-MAP’s ability to make performant decisions in stochastic environments, we compare it with One Risk to Rule Them All (1R2R; Rigter et al. (2023)), a risk-averse model-based algorithm designed for stochastic domains, and model-free actor-critic methods Conservative Q-Learning (CQL; Kumar et al. (2020)) and Implicit Q-Learning (IQL; Kostrikov et al. (2022)). We evaluate L-MAP on Stochastic MuJoCo tasks (Rigter et al., 2023), which serve as a proof of concept in the stochastic continuous control domain.

We then test L-MAP on Adroit, which presents a challenge with its high state and action dimensionality. Finally, we evaluate L-MAP on AntMaze, a sparse-reward continuous-control problem. In this task, L-MAP achieves similar performance to TT, surpassing model-free methods. Through these diverse evaluations, we aim to demonstrate L-MAP’s versatility and effectiveness across different types of control problems, including stochastic environments, high-dimensional spaces, and sparse-reward scenarios. Additionally, we conduct an ablation study to analyze the impact of key components in L-MAP; detailed results of this study can be found in Appendix A.

**Hyperparameters** As for the L-MAP-specific hyperparameters, we set our macro action length to 3. The planning horizon in the raw action space is set to 9 for gym locomotion tasks and 15 for Adroit tasks. These horizons are either smaller or equal to those used in TT and TAP. Our choice of parameters is to ensure a control rate of approximately 10 Hz for locomotion tasks. For each task, we conduct experiments with 3 different training seeds, and each seed is evaluated for 20 episodes.

**Stochastic Mujoco** On the Stochastic MuJoCo tasks, with results presented in Table 1, L-MAP **consistently outperforms the model-based baselines, TAP and TT, across all datasets and environments**, demonstrating its superior capacity to handle stochasticity in continuous control tasks. Notably, L-MAP achieves the highest performance in multiple datasets for both the Hopper and Walker2D environments. When compared to 1R2R, a risk-averse model-based algorithm specifically designed for stochastic domains, L-MAP shows competitive or superior results in most cases. An exception is the Medium-Replay-High Hopper dataset, where 1R2R attains a higher score. This suggests that while L-MAP exhibits robustness across a variety of stochastic settings, there are specific scenarios where risk-averse strategies like 1R2R may hold an advantage. Additionally, L-MAP generally outperforms the model-free methods, CQL and IQL. However, CQL surpasses L-MAP in the Medium-Expert-Mod Hopper dataset. It is worth noting that L-MAP is the only method among all baselines that achieves performance comparable to CQL in this specific setting.

Table 1: Results for Stochastic MuJoCo.

Dataset Type	Env	Model-Based				Model-Free	
		L-MAP	TAP	TT	1R2R	CQL	IQL
Medium-Expert-Mod	Hopper	106.11 ± 2.16	40.86 ± 5.42	56.10 ± 3.33	52.19 ± 8.37	<b>106.17 ± 2.16</b>	60.61 ± 3.46
Medium-Expert-Mod	Walker2D	<b>93.43 ± 1.41</b>	91.40 ± 1.42	80.93 ± 2.60	56.48 ± 7.51	91.44 ± 1.44	86.66 ± 1.84
Medium-Mod	Hopper	55.07 ± 3.06	43.64 ± 2.25	44.49 ± 2.47	<b>65.24 ± 3.31</b>	49.92 ± 3.00	56.00 ± 3.60
Medium-Mod	Walker2D	52.94 ± 1.57	44.46 ± 1.82	43.61 ± 2.15	<b>65.16 ± 2.84</b>	49.38 ± 2.02	48.82 ± 2.31
Medium-Replay-Mod	Hopper	<b>52.30 ± 2.65</b>	38.10 ± 3.22	37.85 ± 1.19	22.82 ± 2.08	40.53 ± 1.52	49.12 ± 3.38
Medium-Replay-Mod	Walker2D	51.44 ± 1.65	43.49 ± 2.27	27.43 ± 3.33	<b>52.23 ± 2.22</b>	40.24 ± 1.67	40.77 ± 2.72
Medium-Expert-High	Hopper	66.93 ± 3.46	37.31 ± 3.66	58.04 ± 3.60	37.99 ± 2.71	<b>68.03 ± 3.94</b>	44.83 ± 2.58
Medium-Expert-High	Walker2D	<b>97.18 ± 2.08</b>	91.09 ± 2.78	50.01 ± 3.51	32.38 ± 4.55	83.18 ± 3.70	68.61 ± 3.33
Medium-High	Hopper	<b>55.32 ± 3.56</b>	43.93 ± 2.66	41.26 ± 5.53	33.99 ± 0.92	45.21 ± 2.97	49.69 ± 2.47
Medium-High	Walker2D	<b>68.87 ± 2.21</b>	52.20 ± 2.76	59.84 ± 5.03	32.13 ± 4.51	61.49 ± 3.24	47.53 ± 3.05
Medium-Replay-High	Hopper	58.05 ± 3.36	48.69 ± 2.97	39.24 ± 2.16	<b>68.25 ± 3.78</b>	51.70 ± 3.09	43.27 ± 2.78
Medium-Replay-High	Walker2D	<b>65.87 ± 3.07</b>	55.15 ± 3.29	16.55 ± 2.17	65.63 ± 3.41	50.33 ± 3.88	45.13 ± 2.38
<b>Mean</b>		<b>68.63</b>	52.53	46.28	48.71	61.47	53.42

**D4RL MuJoCo** On the deterministic MuJoCo tasks, particularly when compared to established model-free approaches such as CQL and IQL, L-MAP demonstrates **notable performance in environments like Walker2D and Hopper**, matching or exceeding these baselines even in dense reward scenarios as shown in Table 2. This highlights L-MAP’s effectiveness across various task structures. When compared to TT, L-MAP consistently delivers comparable results. However, L-

MAP offers a significant practical advantage: its use of **temporal abstraction enables lower latency decision-making for equivalent planning horizons**, resulting in improved efficiency during deployment. Furthermore, L-MAP generally outperforms TAP, suggesting that even in deterministic environments, the expectation-based planning approach proves advantageous by accounting for stochasticity in the behavior policy. This leads to more robust policies and, consequently, superior results.

Table 2: Normalised results for D4RL MuJoCo-v2 following the protocol of Fu et al. (2020)

Dataset Type	Env	Model-Based				Model-Free	
		L-MAP	TAP	TT	1R2R	CQL	IQL
Medium-Expert	HalfCheetah	92.14 ± 0.26	86.40 ± 2.22	<b>95.0 ± 0.2</b>	93.99 ± 1.40	91.6	86.7
Medium-Expert	Hopper	105.74 ± 2.24	85.55 ± 3.83	<b>110.0 ± 2.7</b>	57.40 ± 6.06	105.4	91.5
Medium-Expert	Walker2D	109.35 ± 0.08	105.32 ± 2.03	101.9 ± 6.8	73.18 ± 6.29	108.8	<b>109.6</b>
Medium	HalfCheetah	45.50 ± 0.10	44.73 ± 0.39	46.9 ± 0.4	<b>73.45 ± 0.15</b>	44.4	47.4
Medium	Hopper	<b>73.90 ± 1.91</b>	69.14 ± 2.33	61.1 ± 3.6	55.49 ± 3.99	58.0	66.3
Medium	Walker2D	<b>80.31 ± 1.20</b>	51.75 ± 3.30	79.0 ± 2.8	55.69 ± 4.97	72.5	78.3
Medium-Replay	HalfCheetah	38.45 ± 0.80	40.83 ± 0.72	41.9 ± 2.5	<b>63.85 ± 0.19</b>	45.5	44.2
Medium-Replay	Hopper	91.18 ± 0.56	80.92 ± 3.79	91.5 ± 3.6	89.67 ± 1.92	<b>95.0</b>	94.7
Medium-Replay	Walker2D	81.04 ± 2.62	72.32 ± 3.26	82.6 ± 6.9	<b>90.67 ± 1.98</b>	77.2	77.2
<b>Mean</b>		<b>79.73</b>	70.77	78.88	72.60	77.60	77.32

**Adroit Control** In the Adroit robotic control tasks, which are characterized by their high-dimensional state and action spaces, our proposed method, L-MAP, **demonstrates strong and competitive performance** as shown in Table 3. Across the Human, Cloned, and Expert datasets, L-MAP exhibits notable effectiveness compared to both model-based approaches (TAP and TT) and model-free methods (CQL, IQL, and Behavior Cloning (BC)<sup>1</sup>).

In the Human dataset, which includes suboptimal human demonstrations, L-MAP achieves the highest score in the Door environment and performs well in other tasks. Although IQL leads in the Pen task and CQL leads in the Hammer and Relocate tasks, L-MAP maintains competitive results, particularly surpassing TT and BC in most environments. This suggests that L-MAP effectively utilizes suboptimal data to make robust decisions in complex settings. For the Cloned dataset, which contains a mix of optimal and suboptimal trajectories, L-MAP secures top performance in the Pen and Relocate tasks. In the Expert dataset, comprised of optimal demonstrations, L-MAP attains the highest scores in the Pen and Relocate environments while remaining competitive in the Hammer and Door tasks. Overall, L-MAP achieves the highest average score of 51.40 across all datasets and environments, and 18.79 across non-expert datasets, highlighting its effectiveness in handling varying levels of data optimality. Furthermore, the experimental results indicate that L-MAP effectively manages the complexities of high-dimensional Adroit environments. Incorporating more action information into the single token does not detract from performance; instead, it appears to enhance the model’s ability to learn nuanced temporal dependencies required for successful task execution.

**AntMaze** In the AntMaze environments—a set of sparse-reward continuous-control tasks where an agent must navigate a robotic ant to a target location, L-MAP demonstrates strong and competitive performance as shown in Table 4. These tasks are particularly challenging due to the sparse rewards and the presence of suboptimal trajectories that lead to various goals other than the target position used during testing.

Similar to TAP, our approach integrates goal positions into the observation space, allowing it to condition trajectory generation on specific goals. This conditioning narrows the focus of sampled trajectories towards the target direction, simplifying the planning process. Instead of using the IQL critic for value estimation, L-MAP leverages Monte Carlo planning to provide refined value estimates. This alternative approach avoids the additional computational cost of sampling with a separate Q-network, as required by TT (+Q).

Our method achieves an average success rate of 83.33% across all AntMaze environments, which is comparable to the 84.00% average of TT (+Q). Notably, L-MAP outperforms TT (+Q) in the

<sup>1</sup>We included Behavior Cloning (BC) as an additional baseline since the original 1R2R method was not evaluated for Adroit tasks.



Table 3: Adroit robotic hand control results.

Dataset Type	Env	Model-Based Approaches			Model-Free Approaches		
		L-MAP	TAP	TT	CQL	IQL	BC
Human	Pen	<b>76.26 ± 8.58</b>	66.86 ± 8.41	36.4	37.5	71.5	34.4
Human	Hammer	1.71 ± 0.12	1.57 ± 0.09	0.8	<b>4.4</b>	1.4	1.5
Human	Door	<b>11.24 ± 1.11</b>	9.51 ± 1.10	0.1	9.9	4.3	0.5
Human	Relocate	0.09 ± 0.02	0.06 ± 0.01	0.0	<b>0.2</b>	0.1	0.0
Cloned	Pen	<b>60.68 ± 7.88</b>	46.44 ± 7.54	11.4	39.2	37.3	56.9
Cloned	Hammer	<b>2.43 ± 0.29</b>	1.32 ± 0.12	0.5	2.1	2.1	0.8
Cloned	Door	13.22 ± 1.34	<b>13.45 ± 1.43</b>	-0.1	0.4	1.6	-0.1
Cloned	Relocate	<b>0.15 ± 0.13</b>	-0.23 ± 0.01	-0.1	-0.1	-0.2	-0.1
Expert	Pen	<b>126.60 ± 5.60</b>	112.16 ± 6.57	72.0	107.0	-	85.1
Expert	Hammer	127.16 ± 0.29	<b>128.79 ± 0.52</b>	15.5	86.7	-	125.6
Expert	Door	105.24 ± 0.10	<b>105.86 ± 0.08</b>	94.1	101.5	-	34.9
Expert	Relocate	<b>107.57 ± 0.76</b>	106.21 ± 1.61	10.3	95.0	-	101.3
<b>Mean (All)</b>		<b>51.40</b>	49.33	20.08	40.32	14.76	36.73
<b>Mean (Non-Expert)</b>		<b>18.79</b>	17.37	6.13	11.70	14.76	11.74

Table 4: Performance comparison on AntMaze environments. This evaluation demonstrates that our approach can achieve comparable performance to TT with a separate Q network, while being more efficient during sampling and decision-making.

Dataset Environment	BC	CQL	IQL	TT (+Q)	TAP	L-MAP
Umaze AntMaze	54.6	74.0	87.5	<b>100.0 ± 0.0</b>	78.33 ± 5.32	93.33 ± 3.22
Medium-Play AntMaze	0.0	61.2	71.2	<b>93.3 ± 6.4</b>	43.33 ± 6.40	75.00 ± 6.85
Medium-Diverse AntMaze	0.0	53.7	70.0	<b>100.0 ± 0.0</b>	30.00 ± 5.92	88.33 ± 4.14
Large-Play AntMaze	0.0	15.8	39.6	66.7 ± 12.2	63.33 ± 6.22	<b>78.33 ± 5.32</b>
Large-Diverse AntMaze	0.0	14.9	47.5	60.0 ± 12.7	66.67 ± 6.09	<b>81.67 ± 5.00</b>
<b>Mean</b>	10.92	43.92	55.16	<b>84.00</b>	56.33	83.33

more complex Large-Play and Large-Diverse environments, achieving success rates of 78.33% and 81.67% respectively, compared to TT (+Q)’s 66.7% and 60.0%. This indicates that L-MAP is particularly effective in larger mazes where navigation complexity is higher. While TT (+Q) attains perfect success rates in smaller environments like Umaze and Medium-Diverse, L-MAP still performs exceptionally well with success rates of 93.33% and 88.33% in these settings. This consistency suggests that our method is robust across different scales of environment complexity.

## 5 RELATED WORK

Recent advancements in reinforcement learning focus on learning temporally extended action primitives to reduce decision-making horizons and improve learning efficiency. Both model-free and model-based methods leverage temporal abstraction to manage task complexity.

Model-free methods such as CompILE (Kipf et al., 2019), RPL (Gupta et al., 2019), OPAL (Ajay et al., 2021), ACT (Zhao et al., 2023), and PRISE (Zheng et al., 2024) leverage temporal abstraction in various ways. For instance, CompILE learns latent codes representing variable-length behavior segments, enabling cross-task generalization. RPL employs a hierarchical policy architecture to simplify long-horizon tasks by decomposing them into sub-policies. OPAL introduces a continuous space of primitive actions to reduce distributional shift in offline RL, enhancing policy robustness. PRISE applies sequence compression to learn variable-length action primitives, improving behavior cloning by capturing essential behavioral patterns. These approaches demonstrate the versatility of temporal abstraction in addressing different challenges in reinforcement learning, particularly in managing the complexity inherent in sequential decision-making.

From a model-based perspective, recent work has treated reinforcement learning as a sequence modeling problem, utilizing Transformer architectures to model entire trajectories of states, actions, rewards, and values. This approach is exemplified by methods like Trajectory Transformer (TT) (Zhou et al., 2020), and TAP (Jiang et al., 2023). TAP, in particular, shares conceptual similarities with

our proposed method, L-MAP, in its use of efficient planning solutions for complex action spaces. These sequence modeling approaches have shown promise in capturing long-term dependencies and handling the variability in trajectories, but they often face challenges in stochastic environments where the outcome is not solely determined by the agent’s actions. As highlighted by Paster et al. (2022), reinforcement learning via supervised learning methods may replicate suboptimal actions that accidentally led to good outcomes due to environmental randomness. To address this issue, they proposed ESPER, a solution inspired by the decision transformer framework (Chen et al., 2021). ESPER mitigates the influence of stochasticity on policy learning in discrete action spaces by clustering trajectories and conditioning on average cluster returns.

From a theoretical perspective, several foundational works have studied continuous-space RL via Hamilton-Jacobi-Bellman equations. For example, Kim et al. (2021) grounded Q-learning and DQN in this theory, characterizing optimal control without explicit optimization, Munos (2000) established convergence results using viscosity solutions, and Han et al. (2017) employed deep learning to solve high-dimensional PDEs via backward stochastic differential equations. While providing crucial theoretical foundations, these works focused on deterministic environments or required perfect knowledge about the dynamics of the environment.

Our approach also has interesting connections to robust RL, though with key distinctions. While robust MDPs (Iyengar, 2005; Nilim & Ghaoui, 2005) deal with varying transition kernels chosen adversarially from uncertainty sets, our work focuses on learning and planning with a fixed transition kernel in an offline setting where environmental stochasticity is captured through learned models. Early robust RL addressed planning with known dynamics in tabular settings (Xu & Mannor, 2010), and generalizing to continuous, high-dimensional spaces is challenging (Lim & Autef, 2019). Our temporal abstraction could complement robust RL by providing structured transition functions, potentially integrating classical robust RL planning into high-dimensional environments.

From a planning perspective, our work relates to methods like MuZero (Schrittwieser et al., 2020), stochastic MuZero (Antonoglou et al., 2022), and Vector Quantized Models for Planning (Ozair et al., 2021), which primarily operate in discrete action spaces and online settings, limiting their applicability to continuous control tasks in offline RL. MuZero Unplugged (Schrittwieser et al., 2021) extended MuZero to the offline setting and adapted to low-dimensional continuous action spaces using factorized policy representations (Tang & Agrawal, 2020). However, scaling to high-dimensional action spaces is challenging due to computational infeasibility and imprecise action selection (Luo et al., 2023). Additionally, MuZero Unplugged focuses on deterministic environments and may struggle in highly stochastic continuous settings.

Our method, L-MAP, extends these concepts to high-dimensional continuous action spaces by effectively handling stochasticity and complexity. Using an encoder to group similar state-macro-action pairs and reconstructing return-to-go estimates via a decoder within the VQ-VAE framework, L-MAP captures essential dynamics while abstracting unnecessary details. This approach models future returns more accurately in stochastic settings. Combined with planning algorithms, L-MAP refines expected return estimates, bridging the gap between temporal abstraction techniques and robust performance in stochastic environments. Our latent code representation and transition model reduce the need to learn separate policy, dynamics, and value components in the offline setting, increasing planning efficiency and accounting for environmental stochasticity, thereby enhancing generalization across complex tasks.

## 6 DISCUSSION AND LIMITATIONS

In conclusion, we introduced the Latent Macro Action Planner (L-MAP), which leverages temporal abstractions learned with a state-conditioned VQ-VAE to construct a discrete latent space of macro-actions. This approach enables efficient planning in high-dimensional continuous action spaces within stochastic environments. Future directions include exploring transfer learning to handle new tasks by training on diverse datasets, and adapting L-MAP to online learning scenarios for continuous improvement to tackle more complex challenges. These efforts aim to enhance generalization and efficiency in complex, real-world settings.

## REFERENCES

- Anurag Ajay, Aviral Kumar, Pulkit Agrawal, Sergey Levine, and Ofir Nachum. OPAL: offline primitive discovery for accelerating offline reinforcement learning. In *9th International Conference on Learning Representations, ICLR 2021, Virtual Event, Austria, May 3-7, 2021*. OpenReview.net, 2021. URL <https://openreview.net/forum?id=V69LGwJ01IN>.
- Robert Almgren and Neil Chriss. Optimal execution of portfolio transactions. *Journal of Risk*, 3: 5–40, 2001.
- Ioannis Antonoglou, Julian Schrittwieser, Sherjil Ozair, Thomas K. Hubert, and David Silver. Planning in stochastic environments with a learned model. In *The Tenth International Conference on Learning Representations, ICLR 2022, Virtual Event, April 25-29, 2022*. OpenReview.net, 2022. URL <https://openreview.net/forum?id=X6D9bAHhBQ1>.
- Wenheng Bao and Xiao-yang Liu. Multi-agent deep reinforcement learning for liquidation strategy analysis. *arXiv preprint arXiv:1906.11046*, 2019.
- Andrew G Barto and Sridhar Mahadevan. Recent advances in hierarchical reinforcement learning. *Discrete event dynamic systems*, 13:341–379, 2003.
- Ashwin Carvalho, Yiqi Gao, Stéphanie Lefèvre, and Francesco Borrelli. Stochastic predictive control of autonomous vehicles in uncertain environments. 2014. URL <https://api.semanticscholar.org/CorpusID:14171346>.
- Lili Chen, Kevin Lu, Aravind Rajeswaran, Kimin Lee, Aditya Grover, Michael Laskin, Pieter Abbeel, Aravind Srinivas, and Igor Mordatch. Decision transformer: Reinforcement learning via sequence modeling. In Marc’Aurelio Ranzato, Alina Beygelzimer, Yann N. Dauphin, Percy Liang, and Jennifer Wortman Vaughan (eds.), *Advances in Neural Information Processing Systems 34: Annual Conference on Neural Information Processing Systems 2021, NeurIPS 2021, December 6-14, 2021, virtual*, pp. 15084–15097, 2021. URL <https://proceedings.neurips.cc/paper/2021/hash/7f489f642a0ddb10272b5c31057f0663-Abstract.html>.
- Adrien Couëtoux, Jean-Baptiste Hoock, Nataliya Sokolovska, Olivier Teytaud, and Nicolas Bonnard. Continuous upper confidence trees. In Carlos A. Coello Coello (ed.), *Learning and Intelligent Optimization - 5th International Conference, LION 5, Rome, Italy, January 17-21, 2011. Selected Papers*, volume 6683 of *Lecture Notes in Computer Science*, pp. 433–445. Springer, 2011. doi: 10.1007/978-3-642-25566-3\_32. URL [https://doi.org/10.1007/978-3-642-25566-3\\_32](https://doi.org/10.1007/978-3-642-25566-3_32).
- Thomas G Dietterich. Hierarchical reinforcement learning with the maxq value function decomposition. *Journal of artificial intelligence research*, 13:227–303, 2000.
- Damien Ernst, Guy-Bart Stan, Jorge Goncalves, and Louis Wehenkel. Clinical data based optimal strategies for hiv: a reinforcement learning approach. *Proceedings of the 45th IEEE Conference on Decision and Control*, pp. 667–672, 2006.
- Justin Fu, Aviral Kumar, Ofir Nachum, George Tucker, and Sergey Levine. D4RL: datasets for deep data-driven reinforcement learning. *CoRR*, abs/2004.07219, 2020. URL <https://arxiv.org/abs/2004.07219>.
- Thomas Gabor, Jan Peter, Thomy Phan, Christian Meyer, and Claudia Linnhoff-Popien. Subgoal-based temporal abstraction in monte-carlo tree search. In Sarit Kraus (ed.), *Proceedings of the Twenty-Eighth International Joint Conference on Artificial Intelligence, IJCAI 2019, Macao, China, August 10-16, 2019*, pp. 5562–5568. ijcai.org, 2019. doi: 10.24963/IJCAI.2019/772. URL <https://doi.org/10.24963/ijcai.2019/772>.
- Abhishek Gupta, Vikash Kumar, Corey Lynch, Sergey Levine, and Karol Hausman. Relay policy learning: Solving long-horizon tasks via imitation and reinforcement learning. In Leslie Pack Kaelbling, Danica Kragic, and Komei Sugiura (eds.), *3rd Annual Conference on Robot Learning, CoRL 2019, Osaka, Japan, October 30 - November 1, 2019, Proceedings*, volume 100 of *Proceedings of Machine Learning Research*, pp. 1025–1037. PMLR, 2019. URL <http://proceedings.mlr.press/v100/gupta20a.html>.

- 594 Jiequn Han, Arnulf Jentzen, and Weinan E. Overcoming the curse of dimensionality: Solving high-  
595 dimensional partial differential equations using deep learning. *CoRR*, abs/1707.02568, 2017.  
596 URL <http://arxiv.org/abs/1707.02568>.
- 597 Ruijie He, Emma Brunskill, and Nicholas Roy. Efficient planning under uncertainty with macro-  
598 actions. *J. Artif. Intell. Res.*, 40:523–570, 2011. doi: 10.1613/JAIR.3171. URL <https://doi.org/10.1613/jair.3171>.
- 600 Thomas Hubert, Julian Schrittwieser, Ioannis Antonoglou, Mohammadamin Barekatain, Simon  
601 Schmitt, and David Silver. Learning and planning in complex action spaces. In Marina Meila  
602 and Tong Zhang (eds.), *Proceedings of the 38th International Conference on Machine Learning,*  
603 *ICML 2021, 18-24 July 2021, Virtual Event*, volume 139 of *Proceedings of Machine Learning Re-*  
604 *search*, pp. 4476–4486. PMLR, 2021. URL <http://proceedings.mlr.press/v139/hubert21a.html>.
- 605 Garud Iyengar. Robust dynamic programming. *Math. Oper. Res.*, 30:257–280, 2005. URL <https://api.semanticscholar.org/CorpusID:6626684>.
- 609 Michael Janner, Qiyang Li, and Sergey Levine. Offline reinforcement learning as one big sequence  
610 modeling problem. In Marc’Aurelio Ranzato, Alina Beygelzimer, Yann N. Dauphin, Percy Liang,  
611 and Jennifer Wortman Vaughan (eds.), *Advances in Neural Information Processing Systems 34:*  
612 *Annual Conference on Neural Information Processing Systems 2021, NeurIPS 2021, December*  
613 *6-14, 2021, virtual*, pp. 1273–1286, 2021. URL <https://proceedings.neurips.cc/paper/2021/hash/099fe6b0b444c23836c4a5d07346082b-Abstract.html>.
- 614 Zhengyao Jiang, Tianjun Zhang, Michael Janner, Yueying Li, Tim Rocktäschel, Edward Grefen-  
615 stette, and Yuandong Tian. Efficient planning in a compact latent action space. In *The*  
616 *Eleventh International Conference on Learning Representations, ICLR 2023, Kigali, Rwanda,*  
617 *May 1-5, 2023*. OpenReview.net, 2023. URL <https://openreview.net/forum?id=cA77NrVEuqn>.
- 618 Jeongho Kim, Jaeuk Shin, and Insoon Yang. Hamilton-jacobi deep q-learning for deterministic  
619 continuous-time systems with lipschitz continuous controls. *J. Mach. Learn. Res.*, 22:206:1–  
620 206:34, 2021. URL <https://jmlr.org/papers/v22/20-1235.html>.
- 621 Thomas Kipf, Yujia Li, Hanjun Dai, Vinícius Flores Zambaldi, Alvaro Sanchez-Gonzalez, Edward  
622 Grefenstette, Pushmeet Kohli, and Peter W. Battaglia. Compile: Compositional imitation learning  
623 and execution. In Kamalika Chaudhuri and Ruslan Salakhutdinov (eds.), *Proceedings of the 36th*  
624 *International Conference on Machine Learning, ICML 2019, 9-15 June 2019, Long Beach, Cali-*  
625 *fornia, USA*, volume 97 of *Proceedings of Machine Learning Research*, pp. 3418–3428. PMLR,  
626 2019. URL <http://proceedings.mlr.press/v97/kipf19a.html>.
- 627 Levente Kocsis and Csaba Szepesvári. Bandit based monte-carlo planning. In Johannes Fürnkranz,  
628 Tobias Scheffer, and Myra Spiliopoulou (eds.), *Machine Learning: ECML 2006, 17th Euro-*  
629 *pean Conference on Machine Learning, Berlin, Germany, September 18-22, 2006, Proceed-*  
630 *ings*, volume 4212 of *Lecture Notes in Computer Science*, pp. 282–293. Springer, 2006. doi:  
631 10.1007/11871842\_29. URL [https://doi.org/10.1007/11871842\\_29](https://doi.org/10.1007/11871842_29).
- 632 Ilya Kostrikov, Ashvin Nair, and Sergey Levine. Offline reinforcement learning with implicit q-  
633 learning. In *The Tenth International Conference on Learning Representations, ICLR 2022, Vir-*  
634 *tual Event, April 25-29, 2022*. OpenReview.net, 2022. URL <https://openreview.net/forum?id=68n2s9ZJWF8>.
- 635 Aviral Kumar, Aurick Zhou, George Tucker, and Sergey Levine. Conservative q-learning for offline  
636 reinforcement learning. In Hugo Larochelle, Marc’Aurelio Ranzato, Raia Hadsell, Maria-Florina  
637 Balcan, and Hsuan-Tien Lin (eds.), *Advances in Neural Information Processing Systems 33: An-*  
638 *ual Conference on Neural Information Processing Systems 2020, NeurIPS 2020, December 6-12,*  
639 *2020, virtual*, 2020. URL <https://proceedings.neurips.cc/paper/2020/hash/0d2b2061826a5df3221116a5085a6052-Abstract.html>.
- 640 Zenan Li, Fan Nie, Qiao Sun, Fang Da, and Hang Zhao. Uncertainty-aware decision transformer  
641 for stochastic driving environments. *CoRR*, abs/2309.16397, 2023. doi: 10.48550/ARXIV.2309.  
642 16397. URL <https://doi.org/10.48550/arXiv.2309.16397>.

- 648 Shiau Hong Lim and Arnaud Autef. Kernel-based reinforcement learning in robust markov decision  
649 processes. In *International Conference on Machine Learning*, 2019. URL [https://api.  
650 semanticscholar.org/CorpusID:174799876](https://api.semanticscholar.org/CorpusID:174799876).
- 651 Jianlan Luo, Perry Dong, Jeffrey Wu, Aviral Kumar, Xinyang Geng, and Sergey Levine. Action-  
652 quantized offline reinforcement learning for robotic skill learning. In Jie Tan, Marc Toussaint,  
653 and Kouros Darvish (eds.), *Conference on Robot Learning, CoRL 2023, 6-9 November 2023,  
654 Atlanta, GA, USA*, volume 229 of *Proceedings of Machine Learning Research*, pp. 1348–1361.  
655 PMLR, 2023. URL <https://proceedings.mlr.press/v229/luo23a.html>.
- 656 Rémi Munos. A study of reinforcement learning in the continuous case by the means of viscosity  
657 solutions. *Mach. Learn.*, 40(3):265–299, 2000. doi: 10.1023/A:1007686309208. URL [https:  
658 //doi.org/10.1023/A:1007686309208](https://doi.org/10.1023/A:1007686309208).
- 659 Arnab Nilim and Laurent El Ghaoui. Robust control of markov decision processes with  
660 uncertain transition matrices. *Oper. Res.*, 53:780–798, 2005. URL [https://api.  
661 semanticscholar.org/CorpusID:1537485](https://api.semanticscholar.org/CorpusID:1537485).
- 662 Sherjil Ozair, Yazhe Li, Ali Razavi, Ioannis Antonoglou, Aäron van den Oord, and Oriol Vinyals.  
663 Vector quantized models for planning. In Marina Meila and Tong Zhang (eds.), *Proceedings of  
664 the 38th International Conference on Machine Learning, ICML 2021, 18-24 July 2021, Virtual  
665 Event*, volume 139 of *Proceedings of Machine Learning Research*, pp. 8302–8313. PMLR, 2021.  
666 URL <http://proceedings.mlr.press/v139/ozair21a.html>.
- 667 Keiran Paster, Sheila A. McIlraith, and Jimmy Ba. You can’t count on luck: Why de-  
668 cision transformers and rvs fail in stochastic environments. In Sanmi Koyejo, S. Mo-  
669 hamed, A. Agarwal, Danielle Belgrave, K. Cho, and A. Oh (eds.), *Advances in Neural  
670 Information Processing Systems 35: Annual Conference on Neural Information Process-  
671 ing Systems 2022, NeurIPS 2022, New Orleans, LA, USA, November 28 - December 9,  
672 2022*, 2022. URL [http://papers.nips.cc/paper\\_files/paper/2022/hash/  
673 fe90657b12193c7b52a3418bdc351807-Abstract-Conference.html](http://papers.nips.cc/paper_files/paper/2022/hash/fe90657b12193c7b52a3418bdc351807-Abstract-Conference.html).
- 674 Marc Rigter, Bruno Lacerda, and Nick Hawes. One risk to rule them all: A risk-sensitive  
675 perspective on model-based offline reinforcement learning. In Alice Oh, Tristan Nau-  
676 mann, Amir Globerson, Kate Saenko, Moritz Hardt, and Sergey Levine (eds.), *Advances  
677 in Neural Information Processing Systems 36: Annual Conference on Neural Informa-  
678 tion Processing Systems 2023, NeurIPS 2023, New Orleans, LA, USA, December 10 - 16,  
679 2023*, 2023. URL [http://papers.nips.cc/paper\\_files/paper/2023/hash/  
680 f49287371916715b9209fa41a275851e-Abstract-Conference.html](http://papers.nips.cc/paper_files/paper/2023/hash/f49287371916715b9209fa41a275851e-Abstract-Conference.html).
- 681 Julian Schrittwieser, Ioannis Antonoglou, Thomas Hubert, Karen Simonyan, Laurent Sifre, Simon  
682 Schmitt, Arthur Guez, Edward Lockhart, Demis Hassabis, Thore Graepel, Timothy P. Lillicrap,  
683 and David Silver. Mastering atari, go, chess and shogi by planning with a learned model. *Nat.*,  
684 588(7839):604–609, 2020. doi: 10.1038/S41586-020-03051-4. URL [https://doi.org/  
685 10.1038/s41586-020-03051-4](https://doi.org/10.1038/s41586-020-03051-4).
- 686 Julian Schrittwieser, Thomas Hubert, Amol Mandhane, Mohammadamin Barekatin, Ioannis  
687 Antonoglou, and David Silver. Online and offline reinforcement learning by planning with a  
688 learned model. In Marc’Aurelio Ranzato, Alina Beygelzimer, Yann N. Dauphin, Percy Liang,  
689 and Jennifer Wortman Vaughan (eds.), *Advances in Neural Information Processing Systems 34:  
690 Annual Conference on Neural Information Processing Systems 2021, NeurIPS 2021, December  
691 6-14, 2021, virtual*, pp. 27580–27591, 2021. URL [https://proceedings.neurips.cc/  
692 paper/2021/hash/e8258e5140317ff36c7f8225a3bf9590-Abstract.html](https://proceedings.neurips.cc/paper/2021/hash/e8258e5140317ff36c7f8225a3bf9590-Abstract.html).
- 693 David Silver, Thomas Hubert, Julian Schrittwieser, Ioannis Antonoglou, Matthew Lai, Arthur Guez,  
694 Marc Lanctot, Laurent Sifre, Dhharshan Kumaran, Thore Graepel, Timothy Lillicrap, Karen Si-  
695 monyan, and Demis Hassabis. Mastering chess and shogi by self-play with a general reinforce-  
696 ment learning algorithm, 2017. URL <https://arxiv.org/abs/1712.01815>.
- 697 Richard S Sutton, Doina Precup, and Satinder Singh. Between mdps and semi-mdps: A frame-  
698 work for temporal abstraction in reinforcement learning. *Artificial intelligence*, 112(1-2):181–  
699 211, 1999.
- 700  
701

- 702 Yunhao Tang and Shipra Agrawal. Discretizing continuous action space for on-policy optimization.  
703 In *The Thirty-Fourth AAAI Conference on Artificial Intelligence, AAAI 2020, The Thirty-Second*  
704 *Innovative Applications of Artificial Intelligence Conference, IAAI 2020, The Tenth AAAI Sympos-*  
705 *ium on Educational Advances in Artificial Intelligence, EAAI 2020, New York, NY, USA, Febru-*  
706 *ary 7-12, 2020*, pp. 5981–5988. AAAI Press, 2020. doi: 10.1609/AAAI.V34I04.6059. URL  
707 <https://doi.org/10.1609/aaai.v34i04.6059>.
- 708 Aäron van den Oord, Oriol Vinyals, and Koray Kavukcuoglu. Neural discrete repre-  
709 sentation learning. In Isabelle Guyon, Ulrike von Luxburg, Samy Bengio, Hanna M.  
710 Wallach, Rob Fergus, S. V. N. Vishwanathan, and Roman Garnett (eds.), *Advances*  
711 *in Neural Information Processing Systems 30: Annual Conference on Neural Infor-*  
712 *mation Processing Systems 2017, December 4-9, 2017, Long Beach, CA, USA*, pp.  
713 6306–6315, 2017. URL [https://proceedings.neurips.cc/paper/2017/hash/](https://proceedings.neurips.cc/paper/2017/hash/7a98af17e63a0ac09ce2e96d03992fbc-Abstract.html)  
714 [7a98af17e63a0ac09ce2e96d03992fbc-Abstract.html](https://proceedings.neurips.cc/paper/2017/hash/7a98af17e63a0ac09ce2e96d03992fbc-Abstract.html).
- 715 Huan Xu and Shie Mannor. Distributionally robust markov decision processes. In John D.  
716 Lafferty, Christopher K. I. Williams, John Shawe-Taylor, Richard S. Zemel, and Aron Cu-  
717 lotta (eds.), *Advances in Neural Information Processing Systems 23: 24th Annual Confer-*  
718 *ence on Neural Information Processing Systems 2010. Proceedings of a meeting held 6-*  
719 *9 December 2010, Vancouver, British Columbia, Canada*, pp. 2505–2513. Curran Asso-  
720 ciates, Inc., 2010. URL [https://proceedings.neurips.cc/paper/2010/hash/](https://proceedings.neurips.cc/paper/2010/hash/19f3cd308f1455b3fa09a282e0d496f4-Abstract.html)  
721 [19f3cd308f1455b3fa09a282e0d496f4-Abstract.html](https://proceedings.neurips.cc/paper/2010/hash/19f3cd308f1455b3fa09a282e0d496f4-Abstract.html).
- 722 Shuo Yang, George J. Pappas, Rahul Mangharam, and Lars Lindemann. Safe perception-based  
723 control under stochastic sensor uncertainty using conformal prediction. In *62nd IEEE Confer-*  
724 *ence on Decision and Control, CDC 2023, Singapore, December 13-15, 2023*, pp. 6072–6078.  
725 IEEE, 2023. doi: 10.1109/CDC49753.2023.10384075. URL [https://doi.org/10.1109/](https://doi.org/10.1109/CDC49753.2023.10384075)  
726 [CDC49753.2023.10384075](https://doi.org/10.1109/CDC49753.2023.10384075).
- 727 Weirui Ye, Shaohuai Liu, Thanard Kurutach, Pieter Abbeel, and Yang Gao. Mastering atari games  
728 with limited data. In Marc’Aurelio Ranzato, Alina Beygelzimer, Yann N. Dauphin, Percy Liang,  
729 and Jennifer Wortman Vaughan (eds.), *Advances in Neural Information Processing Systems 34:*  
730 *Annual Conference on Neural Information Processing Systems 2021, NeurIPS 2021, December*  
731 *6-14, 2021, virtual*, pp. 25476–25488, 2021. URL [https://proceedings.neurips.cc/](https://proceedings.neurips.cc/paper/2021/hash/d5eca8dc3820cad9fe56a3bafda65ca1-Abstract.html)  
732 [paper/2021/hash/d5eca8dc3820cad9fe56a3bafda65ca1-Abstract.html](https://proceedings.neurips.cc/paper/2021/hash/d5eca8dc3820cad9fe56a3bafda65ca1-Abstract.html).
- 733 Tony Z. Zhao, Vikash Kumar, Sergey Levine, and Chelsea Finn. Learning fine-grained bimanual  
734 manipulation with low-cost hardware. In Kostas E. Bekris, Kris Hauser, Sylvia L. Herbert, and  
735 Jingjin Yu (eds.), *Robotics: Science and Systems XIX, Daegu, Republic of Korea, July 10-14,*  
736 *2023, 2023*. doi: 10.15607/RSS.2023.XIX.016. URL [https://doi.org/10.15607/RSS.](https://doi.org/10.15607/RSS.2023.XIX.016)  
737 [2023.XIX.016](https://doi.org/10.15607/RSS.2023.XIX.016).
- 738 Ruijie Zheng, Ching-An Cheng, Hal Daumé III, Furong Huang, and Andrey Kolobov. PRISE: Ilm-  
739 style sequence compression for learning temporal action abstractions in control. In *Forty-first*  
740 *International Conference on Machine Learning, ICML 2024, Vienna, Austria, July 21-27, 2024.*  
741 *OpenReview.net, 2024*. URL <https://openreview.net/forum?id=p225Od0aYt>.
- 742 Wenxuan Zhou, Sujay Bajracharya, and David Held. PLAS: latent action space for offline rein-  
743 forcement learning. In Jens Kober, Fabio Ramos, and Claire J. Tomlin (eds.), *4th Conference*  
744 *on Robot Learning, CoRL 2020, 16-18 November 2020, Virtual Event / Cambridge, MA, USA,*  
745 *volume 155 of Proceedings of Machine Learning Research*, pp. 1719–1735. PMLR, 2020. URL  
746 <https://proceedings.mlr.press/v155/zhou21b.html>.  
747  
748  
749  
750  
751  
752  
753  
754  
755



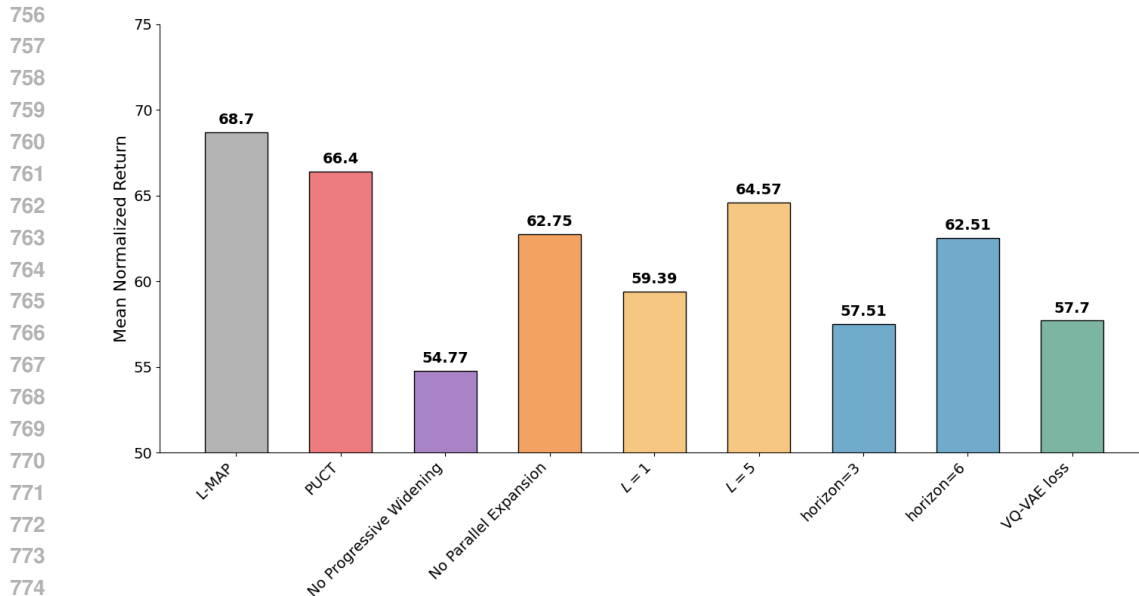


Figure 5: Results of ablation studies, where the height of the bar is the mean normalized scores on high noise gym locomotion control tasks.

## A ABLATION STUDY

We present analyses and ablations of key hyperparameters such as macro action length, planning horizon, the use of pUCT (Silver et al., 2017) versus UCT, and the effect of our customized VQ-VAE loss function. Figure 5 summarizes the results from ablation studies conducted on high-noise stochastic MuJoCo tasks.

### Macro Action Length

We tested macro action lengths  $L = 1$ ,  $L = 3$ , and  $L = 5$  to evaluate their impact on L-MAP’s performance. The highest mean score of 68.7 was achieved with  $L = 3$ . Increasing  $L$  to 5 reduced the mean score to 64.57, while decreasing it to 1 further dropped it to 59.39. This indicates that a macro action length of 3 optimally balances temporal abstraction and adaptability. A moderate length allows the model to capture important action sequences while remaining responsive to environmental changes. Shorter lengths may fail to model temporal dependencies effectively, while longer lengths may hinder quick adaptation in stochastic environments.

### Planning Horizon

We assessed the effect of planning horizon by varying the number of planning steps in L-MAP. Reducing the planning horizon to 3 steps (expanding a single latent variable) decreased the mean score to 57.51, compared to 68.7 with the default longer planning horizon. This demonstrates that a longer planning horizon significantly enhances performance by enabling the model to better anticipate future events and handle uncertainty in high-noise stochastic environments.

### Tree Search Algorithm: UCT vs. pUCT

We compared standard UCT and pUCT as tree search algorithms in L-MAP. UCT achieved a mean score of 68.7, slightly outperforming pUCT, which scored 66.4. While both methods are effective, UCT performs marginally better in this context. A possible explanation is that pUCT leverages a learned prior policy to guide exploration, making it sensitive to the quality of the prior. If the prior policy is suboptimal, pUCT may be less effective due to this dependency.

**VQ-VAE Loss Function** We compared our loss function with the standard loss function without masking (mean scores: 68.7 vs 57.7). Our approach outperforms the standard loss by focusing primarily on state and action during vector quantization. This results in less skewed reconstructed

returns and a more coherent latent space, accurately capturing action and state distributions. Consequently, the model generates more reliable latent representations for reconstruction.

### Progressive Widening

We evaluated the impact of progressive widening on MAP’s performance. Removing progressive widening led to a significant drop in the mean score from 68.70 to 54.77. This substantial decrease demonstrates the importance of controlled state space expansion during planning for a large search space. Progressive widening enables MAP to balance between exploiting existing states in the pre-built search space and incrementally adding new states. Without progressive widening, the search suffers from excessive branching, making it difficult to build sufficiently deep trees for meaningful planning in areas of high stochasticity.

### Parallel Expansion

We assessed the contribution of parallel expansion by comparing L-MAP’s performance with and without this feature. Removing parallel expansion reduced the mean score from 68.7 to 62.75, yielding performance similar to reducing the planning horizon to six steps. This comparison reveals that parallel expansion primarily affects the algorithm’s ability to efficiently explore the search space. Given the same number of MCTS iterations, removing parallel expansion results in less exploration of possible trajectories, reducing the algorithm’s planning capability to that of a shorter horizon. This demonstrates that parallel expansion is crucial for maximizing the effectiveness of each MCTS iteration by enabling broader simultaneous exploration of potential outcomes.

## B ADDITIONAL STOCHASTIC ENVIRONMENT EXPERIMENTS: HIV TREATMENT AND CURRENCY EXCHANGE

Table 5: Results for HIV Treatment and Currency Exchange.

Env	Model-Based Approaches				Model-Free Approaches	
	L-MAP	TAP	TT	1R2R	CQL	IQL
HIV	59.08 ± 1.96	54.95 ± 1.98	54.46 ± 3.30	56.45 ± 2.17	<b>59.74 ± 1.11</b>	34.1 ± 1.2
Currency	<b>106.78 ± 5.00</b>	89.72 ± 3.90	79.28 ± 2.61	78.52 ± 2.08	93.96 ± 1.69	89.41 ± 2.83

The HIV Treatment environment, originally introduced by Ernst et al. (2006), simulates treatment planning where an agent controls two drug types (RTI and PI) in a 6-dimensional state space representing cell and virus concentrations. The stochasticity arises from varying drug efficacy at each step. The Currency Exchange environment, based on the Optimal Liquidation problem (Almgren & Chriss, 2001; Bao & Liu, 2019), involves converting currency under stochastic exchange rates that follow an Ornstein-Uhlenbeck process. Both environments were adapted by Rigter et al. (2023) to the offline RL setting, with datasets collected using partially trained and random policies respectively.

For the HIV Treatment domain, L-MAP and CQL achieve comparable strong performance (59.08 ± 1.96 and 59.74 ± 1.11 respectively), outperforming other baselines. In the Currency Exchange environment, L-MAP substantially outperforms all other approaches, achieving a score of 106.78 ± 5.00 compared to the next best performer CQL at 93.96 ± 1.69. This superior performance demonstrates L-MAP’s versatility across different types of stochastic environments.

## C LATENT SPACE ANALYSIS

To empirically demonstrate the uncertainties introduced by non-injective mappings, behavior policy, and environmental stochasticity, we generate heatmaps representing the transition probabilities between latent codes. We focus on the Hopper environment and consider three datasets: `medium-expert`, `medium`, and `medium-replay`, in both deterministic and stochastic settings. The heatmaps are constructed by encoding the state-macro-action pairs into latent codes using our learned representation and visualizing the transition probabilities between these codes.

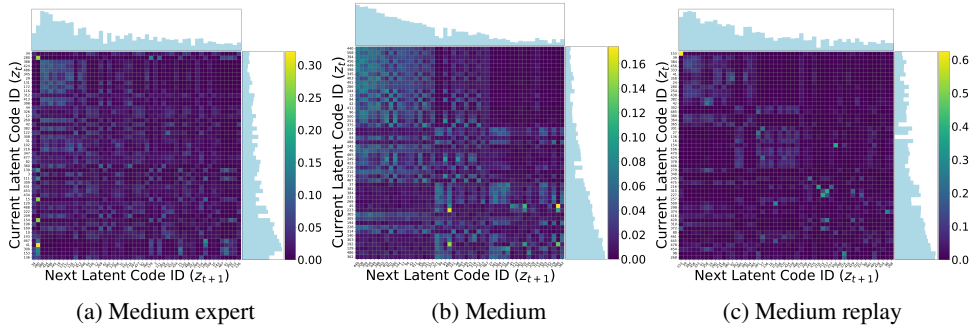


Figure 6: Heatmaps for Deterministic Hopper Environment (Top 50 Frequent Latent Codes). In each heatmap, the intensity of the color at position  $(i, j)$  represents the probability of transitioning from the current latent code  $z_t = i$  to the next latent code  $z_{t+1} = j$ . The accompanying histograms display the frequency of each latent code occurring across the dataset with the learned encoder as the current ( $z_t$ , right histogram) and next ( $z_{t+1}$ , top histogram) codes. The observed spread in the heatmaps indicates that, despite the deterministic nature of the environment, transitions from a single  $z_t$  lead to multiple  $z_{t+1}$ .

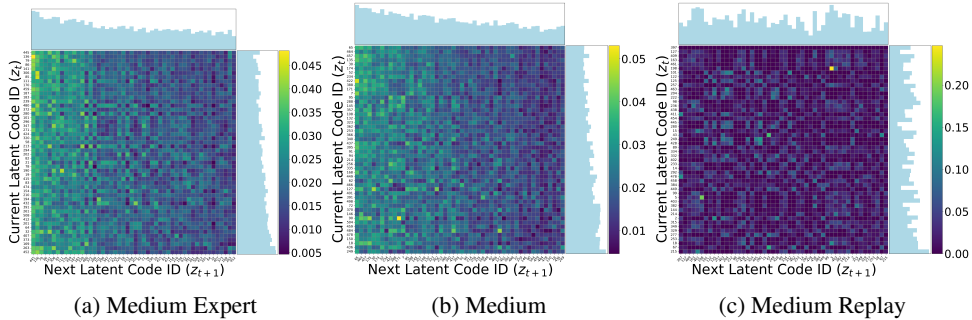


Figure 7: Heatmaps for Stochastic Hopper Environment (Top 50 Frequent Latent Codes). The observed spread in the heatmaps indicates that inherent environmental stochasticity further contributes to transitions from a single  $z_t$  leading to multiple  $z_{t+1}$ .

### C.1 DETERMINISTIC ENVIRONMENT HEATMAPS

In analyzing the heatmaps for deterministic environments as shown in Fig. 6, it becomes evident that transitions from a current latent code  $z_t$  to multiple next latent codes  $z_{t+1}$  are not strictly deterministic. This observed spread in transitions originates from two primary sources: the **non-injective nature of the learned representation** and the **stochasticity of the behavior policy** employed during data collection.

First, the **non-injective mapping** of the encoder function  $f_{\text{enc}}$  may result in multiple distinct high-dimensional state-macro-action pairs being mapped to the same latent code as shown in the histograms of Fig.6. Specifically, for different state-macro-action pairs  $x_t^{(1)} = (s_t^{(1)}, m_t^{(1)})$  and  $x_t^{(2)} = (s_t^{(2)}, m_t^{(2)})$ , it is possible that:

$$f_{\text{enc}}(x_t^{(1)}) = f_{\text{enc}}(x_t^{(2)}) = z_t,$$

even though  $x_t^{(1)} \neq x_t^{(2)}$ . Consequently, their corresponding next state-macro-action pairs  $x_{t+1}^{(1)}$  and  $x_{t+1}^{(2)}$  may differ, potentially leading to different next latent codes upon encoding:

$$z_{t+1}^{(1)} = f_{\text{enc}}(x_{t+1}^{(1)}), \quad z_{t+1}^{(2)} = f_{\text{enc}}(x_{t+1}^{(2)}), \quad \text{with } z_{t+1}^{(1)} \neq z_{t+1}^{(2)}.$$

Second, because the **behavior policy**  $\pi_b$  used for data collection may be stochastic, it introduces variability in the selection of macro-actions at both the current and subsequent time steps. Given a

state  $s_t$ , the behavior policy determines the macro-action  $m_t$  as follows:

$$m_t \sim \pi_b(m | s_t).$$

This stochastic selection can result in different macro-actions  $m_t^{(1)}$  and  $m_t^{(2)}$  being chosen from the same state  $s_t$ , which naturally introduces stochasticity. Note that even if the encoder maps both  $x_t^{(1)} = (s_t, m_t^{(1)})$  and  $x_t^{(2)} = (s_t, m_t^{(2)})$  to the same latent code  $z_t$ :

$$f_{\text{enc}}(x_t^{(1)}) = f_{\text{enc}}(x_t^{(2)}) = z_t.$$

the next states  $s_{t+1}^{(1)}$  and  $s_{t+1}^{(2)}$  might differ, even though the environment dynamics  $T_{\text{env}}$  are deterministic, i.e.,

$$s_{t+1}^{(1)} = T_{\text{env}}(s_t, m_t^{(1)}), \quad s_{t+1}^{(2)} = T_{\text{env}}(s_t, m_t^{(2)}), \quad \text{with } s_{t+1}^{(1)} \neq s_{t+1}^{(2)}.$$

These different next states lead to different next state-macro-action pairs:

$$x_{t+1}^{(1)} = (s_{t+1}^{(1)}, m_{t+1}^{(1)}), \quad x_{t+1}^{(2)} = (s_{t+1}^{(2)}, m_{t+1}^{(2)}).$$

Upon encoding, they may yield different next latent codes:

$$z_{t+1}^{(1)} = f_{\text{enc}}(x_{t+1}^{(1)}), \quad z_{t+1}^{(2)} = f_{\text{enc}}(x_{t+1}^{(2)}), \quad \text{with } z_{t+1}^{(1)} \neq z_{t+1}^{(2)}.$$

Therefore, even in a deterministic environment, the combination of a non-injective encoder and a stochastic behavior policy introduces variability in the latent transitions. The heatmaps for deterministic environments empirically demonstrate this spread, showing that each  $z_t$  does not map deterministically to a single  $z_{t+1}$  but rather to a distribution of possible next latent codes.

### C.2 STOCHASTIC ENVIRONMENT HEATMAPS

The heatmaps for stochastic environments as shown in Fig. 7 exhibit a more pronounced spread in transition probabilities. This inherent environmental stochasticity means that for a given  $s_t$  and  $m_t$ , there are multiple possible next states  $s_{t+1}$ , leading to a wider distribution of next latent codes  $z_{t+1}$  upon encoding. When combined with the non-injective mapping of the encoder and the stochasticity of the behavior policy, the uncertainties in the latent transitions are further amplified.

### C.3 THE IMPACT OF $L_1$ REGULARIZATION ON REPRESENTATION FIDELITY

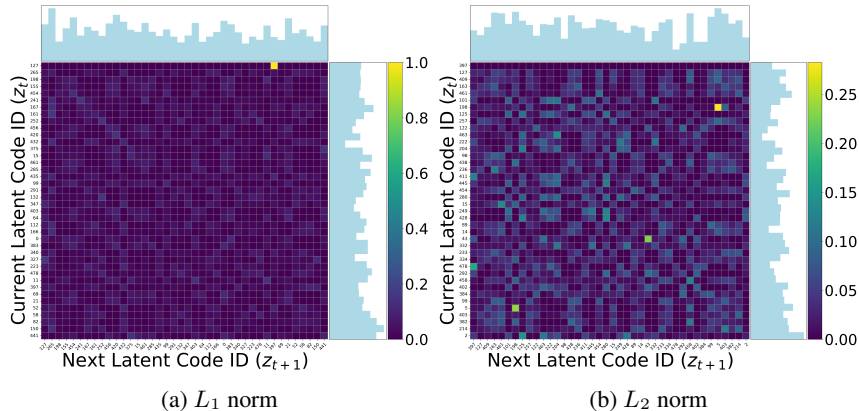


Figure 8: Transition Probability Heatmaps for Medium-Replay Datasets from the Stochastic Hopper Environment (Top 50 Frequent Latent Codes). Left: Heatmap depicting transition probabilities when embeddings are regularized using the  $L_1$  norm. Right: Heatmap illustrating transition probabilities under  $L_2$  norm regularization.

The heatmaps shown in Fig.8 reveal distinct patterns between transition probabilities for latent codes encoded by encoders trained with  $L_1$  and  $L_2$  norm regularization in the latent space. The  $L_2$  norm

demonstrates more distributed transition probabilities, with multiple moderate-probability transitions (shown as light blue dots) for each current state, indicating the encoder preserves more granular information. In contrast, the  $L_1$  norm exhibits highly deterministic transitions for certain latent codes, shown by the predominantly dark purple background with the bright yellow spot approaching probability 1.0. This suggests that the encoder trained with  $L_1$  regularization tends to collapse dissimilar inputs into the same latent code, leading to less nuanced representations.

## D ANALYSIS OF PERFORMANCE TRENDS WITH INCREASING STOCHASTICITY

Table 6: Hopper Environment Results with Increasing Stochasticity

Dataset Type	Env	Model-Based				Model-Free	
		L-MAP	TAP	TT	1R2R	CQL	IQL
<b>Deterministic</b>							
Medium-Expert	Hopper	105.74 ± 2.24	85.55 ± 3.83	<b>110.0 ± 2.7</b>	57.40 ± 6.06	105.4	91.5
Medium	Hopper	<b>73.90 ± 1.91</b>	69.14 ± 2.33	61.1 ± 3.6	55.49 ± 3.99	58.0	66.3
Medium-Replay	Hopper	91.18 ± 0.56	80.92 ± 3.79	91.5 ± 3.6	89.67 ± 1.92	95.0	94.7
<b>Mean (Deterministic)</b>		<b>90.27</b>	78.54	87.53	67.52	86.13	84.17
<b>Moderate Stochasticity</b>							
Medium-Expert-Mod	Hopper	106.11 ± 2.16	40.86 ± 5.42	56.10 ± 3.33	52.19 ± 8.37	<b>106.17 ± 2.16</b>	60.61 ± 3.46
Medium-Mod	Hopper	55.07 ± 3.06	43.64 ± 2.25	44.49 ± 2.47	<b>65.24 ± 3.31</b>	49.92 ± 3.00	56.00 ± 3.60
Medium-Replay-Mod	Hopper	<b>52.30 ± 2.65</b>	38.10 ± 3.22	37.85 ± 1.19	22.82 ± 2.08	40.53 ± 1.52	49.12 ± 3.38
<b>Mean (Moderate Stochasticity)</b>		<b>71.16</b>	40.87	46.15	46.75	65.54	55.24
<b>High Stochasticity</b>							
Medium-Expert-High	Hopper	66.93 ± 3.46	37.31 ± 3.66	58.04 ± 3.60	37.99 ± 2.71	<b>68.03 ± 3.94</b>	44.83 ± 2.58
Medium-High	Hopper	<b>55.32 ± 3.56</b>	43.93 ± 2.66	41.26 ± 5.53	33.99 ± 0.92	45.21 ± 2.97	49.69 ± 2.47
Medium-Replay-High	Hopper	58.05 ± 3.36	48.69 ± 2.97	39.24 ± 2.16	<b>68.25 ± 3.78</b>	51.70 ± 3.09	43.27 ± 2.78
<b>Mean (High Stochasticity)</b>		<b>60.10</b>	43.31	46.18	46.74	54.98	45.93

This section examines how L-MAP and baseline methods respond to increasing levels of stochasticity in the Hopper environment. Table 6 presents the performance metrics across deterministic, moderate, and high stochasticity settings.

In the **deterministic** setting, L-MAP achieves a mean score of **90.27**, indicating strong performance and outperforming all other model-based methods. Among the baselines, TT attains a mean of 87.53, TAP achieves 78.54, and 1R2R scores 67.52. The model-free methods CQL and IQL also perform well, with mean scores of 86.13 and 84.17, respectively. The high scores across all methods suggest that the deterministic environment poses minimal challenges, allowing both L-MAP and the baselines to excel.

As the environment introduces **moderate stochasticity**, L-MAP’s mean performance decreases to **71.16**, reflecting a reduction of approximately 21% from its deterministic performance. The model-based baselines experience larger declines; TAP’s mean drops to 40.87 (a 48% reduction), TT’s to 46.15 (a 47% reduction), and 1R2R’s to 46.75 (a 31% reduction). The model-free methods also suffer performance losses; CQL’s mean decreases to 65.54 (a 24% reduction), and IQL’s to 55.24 (a 34% reduction). Despite the reductions, L-MAP maintains a higher mean score than all baselines in this setting, indicating better resilience to moderate stochasticity among both model-based and model-free methods.

In the setting of **high stochasticity**, L-MAP’s mean further decreases to **60.10**, representing a total reduction of about 33% from the deterministic case. The model-based baselines continue to show declining trends; TAP’s mean falls to 43.31 (a 45% reduction), TT’s to 46.18 (a 47% reduction), and 1R2R’s to 46.74 (a 31% reduction). The model-free methods also see further decreases; CQL’s mean drops to 54.98 (a 36% reduction), and IQL’s to 45.93 (a 45% reduction). While all methods experience performance degradation, L-MAP consistently outperforms the model-based baselines TAP and TT, and maintains an edge over the model-free methods CQL and IQL. The performance of L-MAP shows relatively better robustness among the baselines.

The overall trend indicates that increasing stochasticity adversely affects all methods, but L-MAP’s performance diminishes at a slower rate compared to the other model-based methods. These results

suggest that L-MAP is more robust to stochastic variations in the environment than most of the baseline methods, particularly the model-based ones.

## E PLANNING HYPERPARAMETERS

For all environments, we utilize the following hyperparameters for sampling during the search process:  $\alpha = 0.1$  and  $\epsilon = 1$ , which determine the exploration rate of progressive widening; and set the number of Monte Carlo Tree Search (MCTS) iterations to 100. Detailed parameters for each environment are presented in Table 7.

Table 7: Planning Hyperparameters

Environment	M	N	B	$\lambda$	$\gamma$
Stochastic MuJoCo	32	4	4	0.5	0.99
D4RL MuJoCo	32	4	4	0.5	0.99
Adroit	10	2	4	0.5	0.99
AntMaze	16	2	4	0.5	0.998
Currency	32	4	4	0.5	0.99
HIV Treatment	5	4	4	1.0	0.99

## F DETAILED DISCUSSION OF KEY METHOD COMPONENTS AND OBJECTIVES

In this section, we provide a comprehensive discussion of the key components of our method and their respective objectives. Each component addresses specific challenges in decision-making within stochastic continuous environments, working together to enable efficient planning.

**Temporal Abstraction (Key Objective: Efficiency and Action Space Reduction).** Macro-actions provide an essential abstraction for managing high-dimensional continuous action spaces by compressing extended action sequences into single units. The latent macro-action space can be significantly smaller than the raw action space since it captures only plausible actions from the dataset, reducing decision complexity while maintaining adaptability.

**Continuous-to-Discrete Mapping (Key Objective: Dimensionality Reduction).** We achieve dimensionality reduction through a state-conditioned VQ-VAE (Vector Quantized Variational Autoencoder). This core component discretizes the continuous state-macro-action space into a discrete latent representation, building on prior works (Jiang et al., 2023; Luo et al., 2023) that recognize learned state-conditioned discretization can maintain high granularity with relatively few discrete actions.

**Latent Prior Model (Key Objective: Efficient Sampling and Transition Modeling).** The learned state-conditioned prior serves dual purposes: efficiently sampling plausible macro-actions and modeling transitions in the latent space, which is crucial for planning initialization.

**Planning (Key Objective: Heuristic Sequential Search in the Latent Space).** We propose a modified Monte Carlo Tree Search (MCTS) algorithm that uses the learned prior to seed the initial search space and employs progressive widening to balance between exploitation of promising actions and exploration of alternatives, enabling effective decision optimization in the latent space.